Pure appl. geophys. 157 (2000) 383–405
0033–4553/00/030383–23 $ 1.50 + 0.20/0

Pure and Applied Geophysics

Comparative Magnetotelluric Modeling of Smooth 2D and 3D Conducting Bodies Using Rayleigh-Fourier Codes

Patricia Martinelli,[1,3] Ana Osella[1,3] and Cristina Pomposiello[2,3]

Abstract—Recently, a method for 3D magnetotelluric modeling was developed, which is based on the application of the Rayleigh scattering theory. This method, RF-3D, is especially capable of modeling multilayered structures with smooth irregular boundaries. The formulation allows inclusion of layers with vertically anisotropic electrical conductivity.

Using RF-3D, the response of smooth structures of practical interest is calculated and the importance of 3D effects is evaluated. Two models consisting of a 3D conductive body in the presence of a 2D shallow distortion are analyzed. In the first model, the direction of maximum elongation of the body is perpendicular to the strike direction of the 2D upper structure, and in the second one both directions coincide. In addition, the case of a small 3D shallow conductor over a regional 2D structure is also considered.

3D effects are compared to those generated by 2D models with identical cross sections. In all the cases, the 3D responses differ from those of the 2D, especially directly over the bodies. A good agreement between the 2D transverse magnetic response and the corresponding components of the 3D response, along centrally located transverse profiles, is expected for elongate, prismatic conductors. Then, the differences obtained for the models considered in this study, particularly for the second and third models, are a consequence of the smooth geometry. They can be explained in terms of galvanic effects produced by boundary charges, which are greater near the vertical sides of a prism than on the sides of a body with smooth contours.

Equivalent 2D models of the first and second structures are also obtained. In these models, the thickness of the conductor is underestimated, respectively, by about 30% and 24%.

For the third model, when vertical anisotropy is analyzed, it is found that only the anisotropy of the first layer can be detected. This is because the effect of vertical anisotropy decreases strongly with depth and appears to be important only near the 3D anomaly.

Key words: 3D magnetotelluric modeling, electrical anisotropy.

Introduction

Improvements in magnetotelluric (MT) data quality have encouraged the application of new methods to interpret the MT impedance tensor in cases where the surveyed structure is not one-dimensional (1D) or two-dimensional (2D). There are

[1] Dto. de Física, Fac. Cs. Exactas y Naturales, Universidad de Buenos Aires, Ciudad Universitaria, Pab. 1-1428, Buenos Aires, Argentina. Fax: 54 1 782-7647. E-mail: osella@df.uba.ar

[2] CIRGEO, Conicet, Ramirez de Velasco 847-1405, Buenos Aires, Argentina.

[3] Also at CONICET (Consejo Nacional de Investigaciones Científicas y Técnicas).

many situations where the conductive structure is approximately 2D; several methods have been developed for these cases, usually using finite elements and finite differences techniques (e.g., WANNAMAKER *et al.*, 1987; SMITH and BOOKER, 1991) or Rayleigh-Fourier expansions (JIRACEK *et al.*, 1989; OSELLA and MARTINELLI, 1993). Although for many studies the 2D modeling can give a realistic interpretation of MT data, even in the presence of three-dimensional (3D) structures, in many cases, 3D structures introduce strong distortions, and therefore, the resulting impedance tensor has a significant 3D behavior. Some methods for 3D modeling have been developed using integral equation approaches (e.g., HOHMANN, 1975; WANNAMAKER, 1991). These methods are especially appropriate when dealing with a few blocks embedded in a 1D layered medium, however they become difficult to apply when the complexity of the structure increases. More recently, 3D algorithms have been proposed which allow modeling of more arbitrarily complex media, using finite differences (MACKIE *et al.*, 1993; SMITH, 1996) and finite elements (MOGI, 1996).

In a previous paper, MARTINELLI and OSELLA (1997) presented an alternative algorithm to model the MT response of 3D structures composed of homogeneous, vertically anisotropic layers with smooth, irregular boundaries, using a modified Rayleigh technique (RF-3D). Rayleigh solutions for the case of isotropic media were previously reported by DANIYAN and PEEPLES (1986) and BOERSMA and JIRACEK (1987).

When dealing with field data, 2D algorithms are commonly used to model the MT response, with diagnostic tests to establish the dimension of the structure (e.g., BAHR, 1988; GROOM and BAILEY, 1989). These methods are satisfactory for superficial anomalous bodies in a 2D regional structure. They do not recover static shift anisotropy, however.

In this paper a study is performed to analyze the importance of 3D effects in the MT response of conductive bodies with smooth contours in the presence of shallow distortions, considering the cases of both embedded and superficial locations.

Methodology

The MT responses are calculated using the RF-3D method, recently developed by MARTINELLI and OSELLA (1997), which has been formulated for modeling N-layered structures with smooth, irregular boundaries, as the one shown in Figure 1. In the following, a brief description of this method is given.

Generally it is assumed that each medium is homogeneous and linear, with magnetic permeability equal to that of the vacuum, μ_0. The possibility of vertical anisotropy of the electrical conductivity is included in the formulation, σ_h and σ_v being, respectively, the conductivities in the horizontal and vertical directions. The coefficient of vertical anisotropy is defined as $\alpha = \sigma_h/\sigma_v$.

The inner boundaries are described by functions $z = S_n(x, y)$ for $1 \leq n < N - 1$, and the air-earth interface is given by $z = 0$. To simplify the treatment, it is presumed that the interfaces $S_n(x, y)$ are even and periodic functions of x and y, their spatial wavelengths being namely λ_x and λ_y. The studied area corresponds to points (x, y) such that $|x - \lambda_x/4| \leq L_x/2$ and $|y - \lambda_y/4| \leq L_y/2$; outside this zone, the interfaces are planar. The effect that the imposed symmetries and periodicities exert over the zone of interest can be reduced by taking λ_x and λ_y much larger than L_x and L_y.

The magnetotelluric response is given by the impedance tensor, $\mathbf{Z}$, and the tipper, $\mathbf{T}$, which relate the values of the components of the electric, $\overline{E}$, and magnetic $\overline{H}$, fields at the earth surface for each frequency, ω. They are defined as:

$$\begin{bmatrix} E_x(x, y, 0, \omega) \\ E_y(x, y, 0, \omega) \end{bmatrix} = \begin{bmatrix} Z_{xx}(x, y, 0, \omega) & Z_{xy}(x, y, 0, \omega) \\ Z_{yx}(x, y, 0, \omega) & Z_{yy}(x, y, 0, \omega) \end{bmatrix} \begin{bmatrix} H_x(x, y, 0, \omega) \\ H_y(x, y, 0, \omega) \end{bmatrix}, \tag{1}$$

$$H_z(x, y, 0, \omega) = T_x(x, y, 0, \omega) H_x(x, y, 0, \omega) + T_y(x, y, 0, \omega) H_y(x, y, 0, \omega). \tag{2}$$

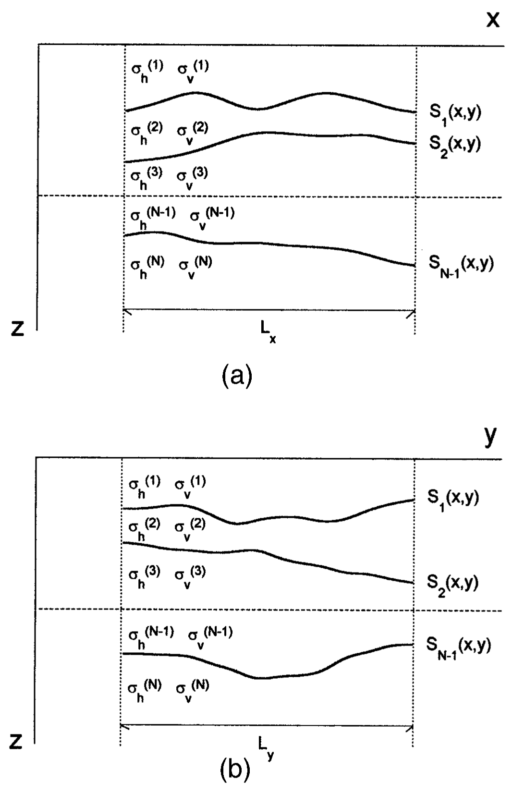

Figure 1
Generalized N-layered model. Interfaces $z = S_n$ are functions of x and y. The electrical conductivity of each medium can be vertically anisotropic.

From each element of $\mathbf{Z}$, Z_{ij}, with $i, j = x, y$, an apparent resistivity is defined as:

$$\rho_{ij}(x, y, 0, \omega) = |Z_{ij}(x, y, 0, \omega)|^2/\omega^2\mu_0. \tag{3}$$

The magnetospheric inducing field is unknown, but can be considered horizontal and spatially uniform (CAGNIARD, 1953). Then, due to the linearity of Maxwell equations, it can be demonstrated that $\mathbf{Z}$ and $\mathbf{T}$ only depend on the characteristics of the structures surveyed and not on the inducing field. They are calculated using two different, linearly polarized external fields, one in the x direction and the other in the y direction.

For a 2D structure with strike direction y, there are two uncoupled modes; the transverse electric mode (TE), with $\overline{E}$ parallel to y, and the transverse magnetic mode (TM), with $\overline{H}$ parallel to y. In this case:

$$Z_{xx} = Z_{yy} = 0, \tag{4}$$

$$Z_{xy} = Z_{TM}, \tag{5}$$

$$Z_{yx} = Z_{TE}, \tag{6}$$

and

$$T_x = T_{TE}, \tag{7}$$

$$T_y = 0. \tag{8}$$

For a general 3D structure, there are no uncoupled modes, and all the elements of $\mathbf{Z}$ and $\mathbf{T}$ are different from 0.

In the RF formalism, the 3D response is calculated applying Rayleigh's scattering theory on every interface. Since some multiple reflections are not included in Rayleigh's formalism, it actually constitutes an approximation. However, this approximation works well in many cases, provided that boundary slopes are not too large (LIPPMANN, 1953; MILLER, 1971). Using this method, structures have been accurately modeled with maximum boundary slopes between 50 and 60 degrees, depending on layer resistivities (MARTINELLI and OSELLA, 1997).

In this work the RF method is applied to calculate the MT response of three different models. Models A and B, which are shown in Figures 2a and 2b, respectively, represent 3D conductive bodies of smooth contours, with 2D shallow (superficial) distortions. In model A, the direction of maximum elongation of the 3D conductor is perpendicular to the strike direction of the 2D upper boundary, while, in model B, both directions are coincident. Model C (see Fig. 3) corresponds to a 2D structure distorted by a shallow, small, 3D conductive body.

The 3D effects are evaluated for each model by comparing its response along two profiles perpendicular to the y direction (one passing just over the center of the conductor and the other passing near its border) to the response of 2D structures with identical x-z cross sections. The y direction corresponds to the superficial strike in models A and B, and to the regional strike in model C.

For models A and B, equivalent 2D models are also obtained for each profile. The structures employed for the forward 2D calculations have the same layer resistivities as models A and B and the same interface S_1; however the interfaces S_2 and S_3 are described by the functions:

$$S_2^{(2D)}(x) = 5 \text{ km} - D/[1 + (x/G)^2], \tag{9}$$

$$S_3^{(2D)}(x) = 5 \text{ km} - D/[1 + (x/G)^2]. \tag{10}$$

Using an iterative trial-and-error procedure, the values of the parameters D and G are varied to find the best fitting between the 3D and 2D responses. For each profile of each model, two equivalent 2D models are obtained; one adjusting the apparent resistivity ρ_{xy} and the phase of Z_{xy}, ϕ_{xy} (TM model), and other adjusting

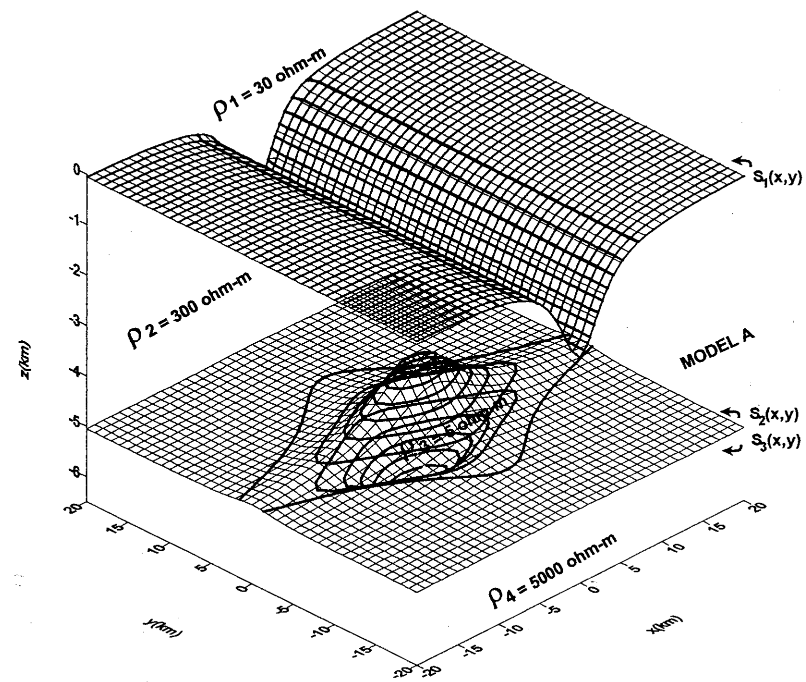

$S_i(x,y) = p_i + d_i/(1 + (x/gx_i)^2)/(1 + (y/gy_i)^2)$

i = 1 to 3; x and y in km

i	p_i(km)	d_i(km)	gx_i(km)	gy_i(km)
1	0	2	3	∞
2	5	-1.5	6	3
3	5	1.5	6	3

(a)

Fig. 2.

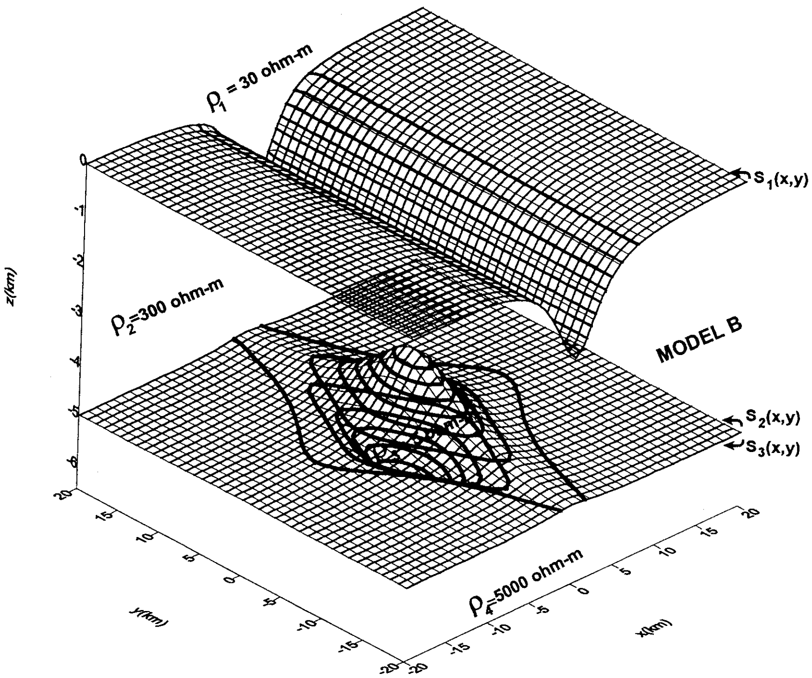

$$S_i\,(x,y) = p_i + d_i\,/(1 + (x/gx_i)^2)/\,(1 + (y/gy_i)^2)$$

i = 1 to 3; x and y in km

i	p_i(km)	d_i(km)	gx_i(km)	gy_i(km)
1	0	2	3	∞
2	5	-1.5	3	6
3	5	1.5	3	6

(b)

Figure 2
3D conducting body of smooth contours underlying a 2D structure, with (a) 3D direction of maximum elongation perpendicular (Model A) and (b) parallel (Model B) to the 2D symmetry axis, respectively.

ρ_{yx} and the phase of Z_{yx}, ϕ_{yx} (TE model). For the 2D responses, ρ_{xy} and ϕ_{xy} correspond to the TM mode and ρ_{yx} and ϕ_{yx} to the TE mode.

In a previous work (Osella and Martinelli, 1993), it was found that the presence of vertical anisotropy in the upper layers can strongly influence the MT response of 2D structures; there, basins and anticlinals were considered. The same seems to be true for 3D cases; in particular, the effect of vertical anisotropy in 3D basins has recently been investigated (Martinelli and Osella, 1997) and the results indicated that this effect decreases strongly with depth. Hence, only the effect of vertical anisotropy for the case of the shallow 3D conductor (model C) is analyzed here.

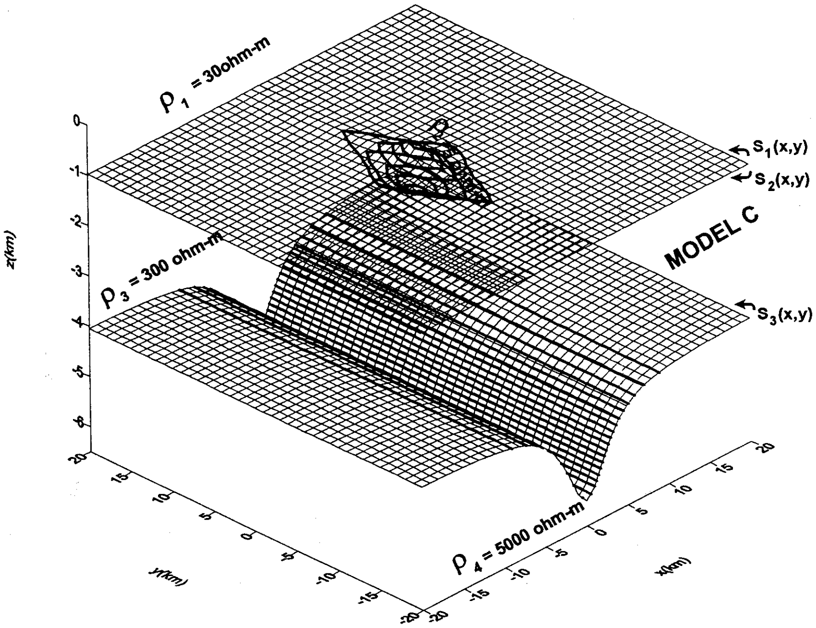

$$S_i(x,y) = p_i + d_i/(1 + (x/gx_i)^2)/(1 + (y/gy_i)^2)$$

i = 1 to 3; x and y in km

i	p_i(km)	d_i(km)	gx_i(km)	gy_i(km)
1	1	-0.5	1.5	3
2	1	0.5	1.5	3
3	4	2	3	∞

Figure 3
2D underlying structure with a shallow, small, 3D conducting body overlying it (Model C).

Results

In this section the main results obtained for each model are summarized.

Model A

As mentioned, two profiles are considered for model A: the profile $y = 0$, which passes over the center of the conducting body (Fig. 4a), and the profile $y = 4$ km (Fig. 5a), which passes near its border.

Profile y = 0—In Figure 4b the apparent resistivities ρ_{xy} and ρ_{yx}, and the phases ϕ_{xy} and ϕ_{yx} corresponding to model A are plotted as functions of the period T, as $y = 0$ km, for different values of x.

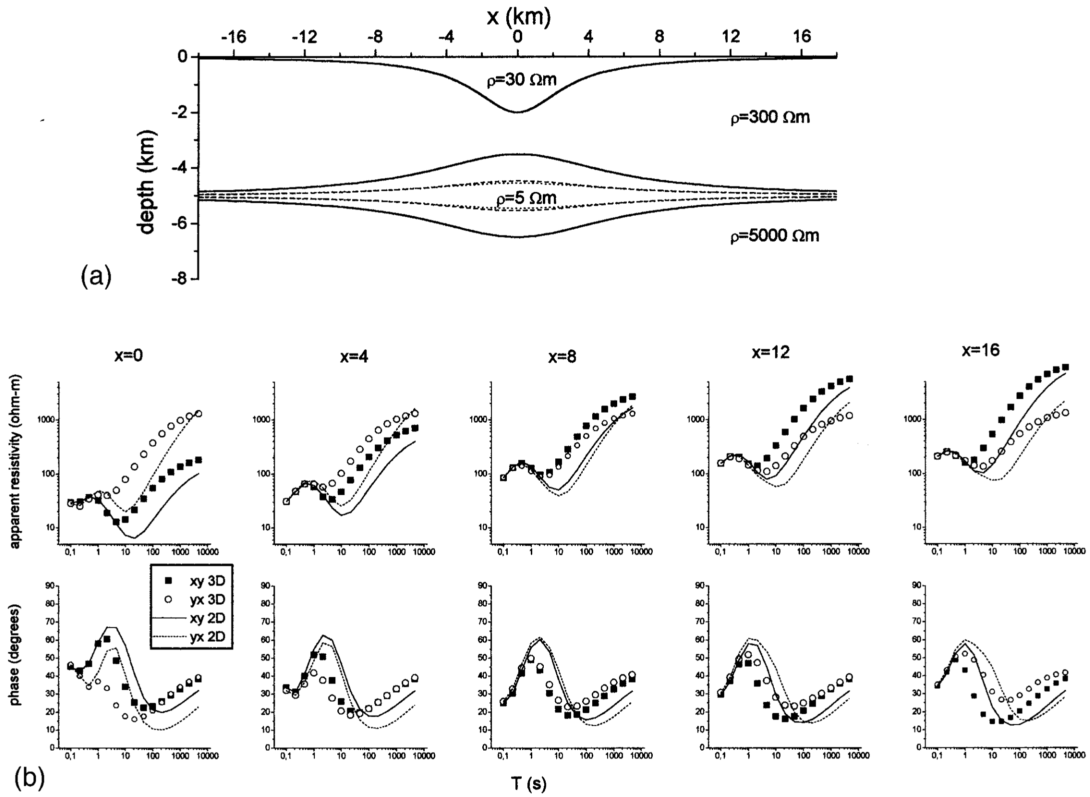

Figure 4

(a) Cross section of Model A at $y = 0$, together with the equivalent 2D models (dashed contours—2D TM model obtained adjusting the 3D xy-component responses; dotted contours—2D TE model obtained adjusting the 3D yx-component responses). (b) 3D apparent resistivity (ρ_{xy} and ρ_{yx}) and phase (ϕ_{xy} and ϕ_{yx}) curves from the corresponding impedance tensor components, at $y = 0$, for different values of x. The responses of a 2D model with the same cross section are also shown. (c) 2D TM model fits of the 3D xy-components. Results for the 2D TE model are similar. (d) Comparison of 3D modulus and phase of T_x, with 2D TE forward responses of the TM and TE models.

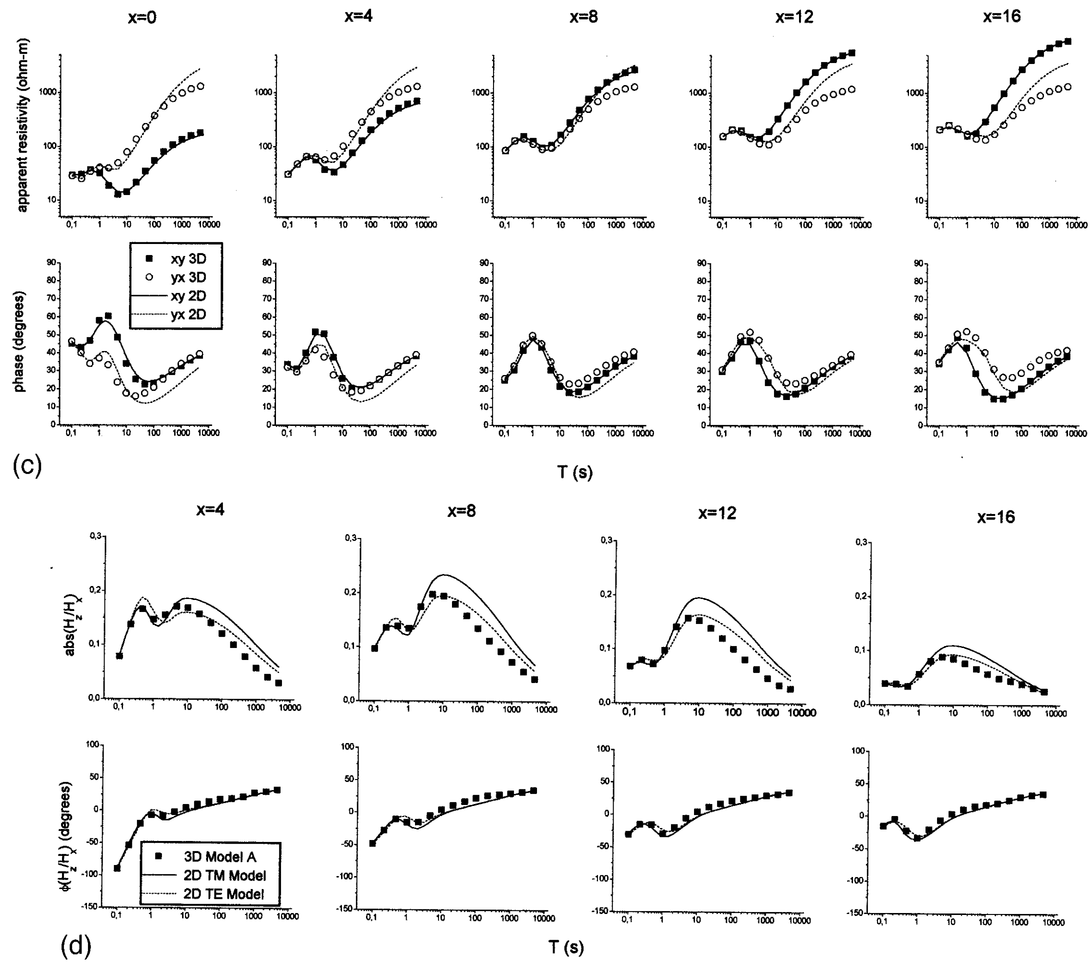

x=0
x=4
x=8
x=12
x=16
apparent resistivity (ohm-m)
phase (degrees)
xy 3D
yx 3D
xy 2D
yx 2D
(c)
T (s)
abs(H_z/H_x)
φ(H_z/H_x) (degrees)
3D Model A
2D TM Model
2D TE Model
(d)
T (s)

Fig. 4.

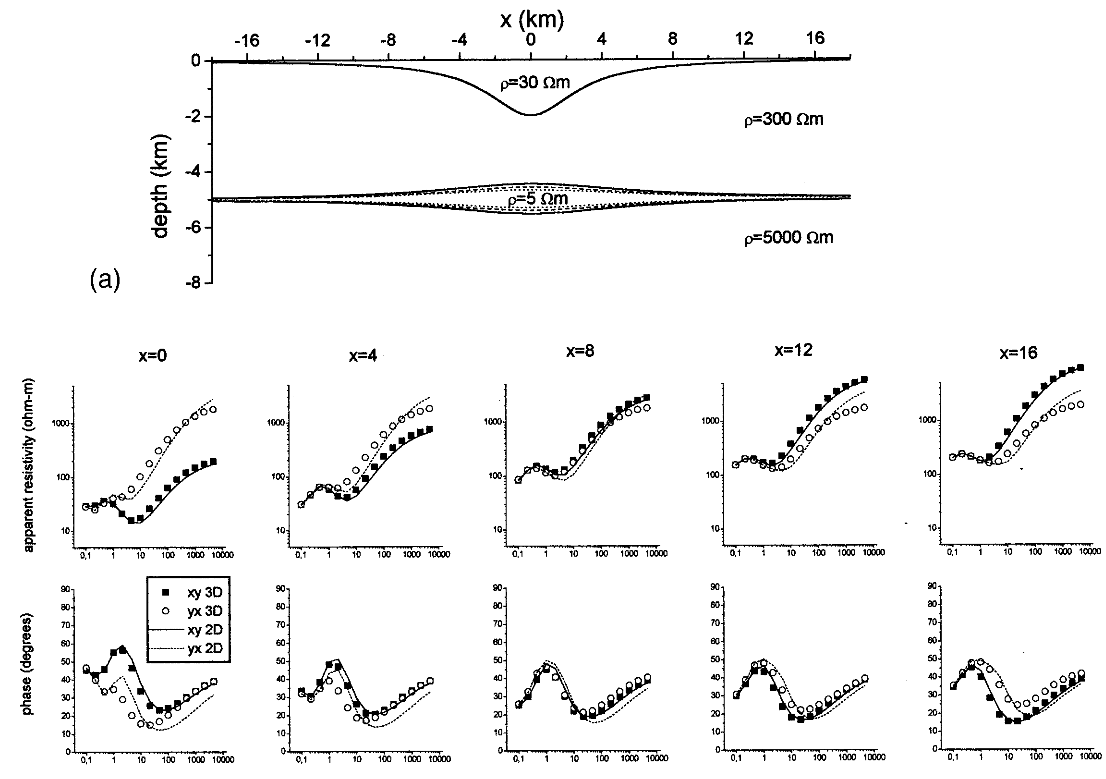

Figure 5

(a) Cross section of Model A at $y = 4$ km, together with the equivalent 2D models (dashed contours—2D TM model obtained adjusting the 3D xy-component responses; dotted contours—2D TE model obtained adjusting the 3D yx-component responses). (b) 3D apparent resistivity (ρ_{xy} and ρ_{yx}) and phase (ϕ_{xy} and ϕ_{yx}) curves from the corresponding impedance tensor components, at $y = 4$ km, for different values of x. The responses of a 2D model with the same cross section are also shown. (c) 2D TM model fits of the 3D xy components. Results for the 2D TE model are similar. (d) Comparison of 3D modulus and phase of T_x, with 2D TE forward responses of the TM and TE models.

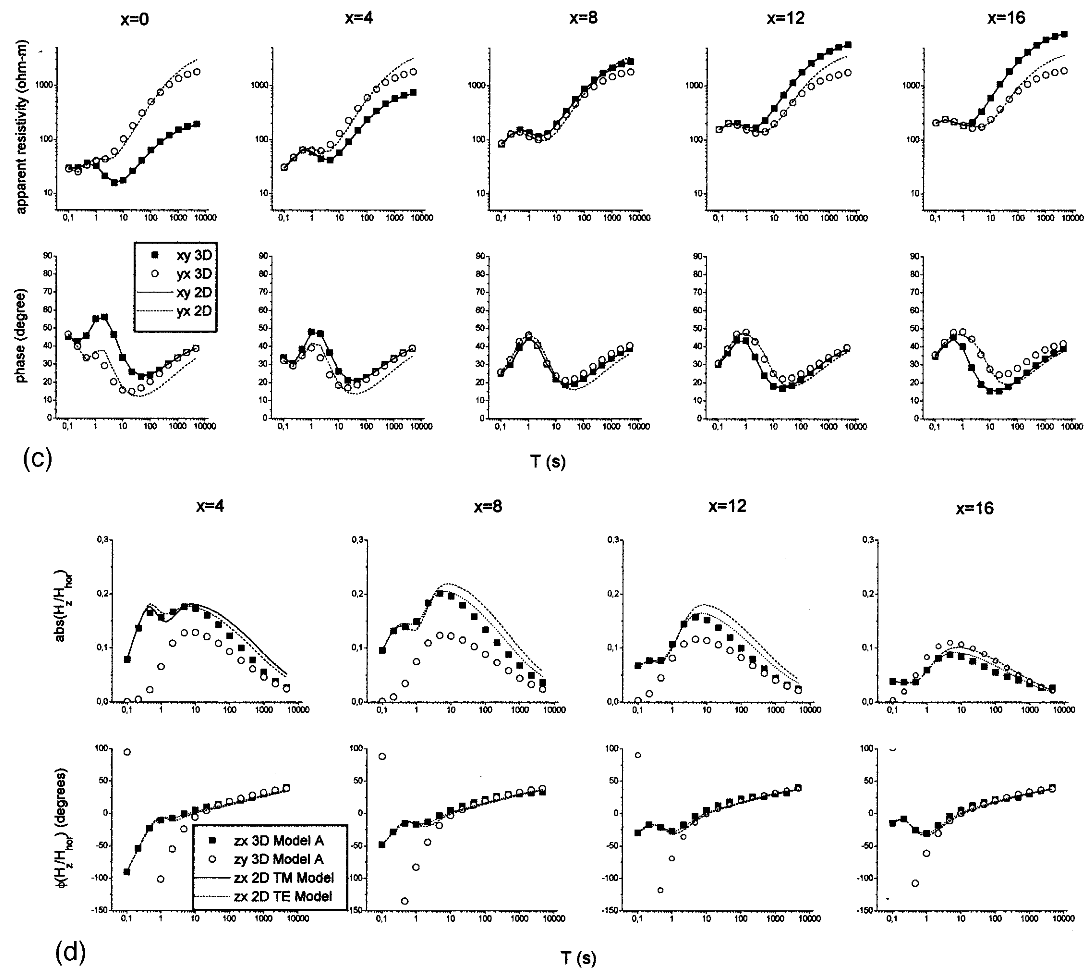
x=0
x=4
x=8
x=12
x=16
apparent resistivity (ohm-m)
phase (degree)
xy 3D
yx 3D
xy 2D
yx 2D
(c)
T (s)
x=4
x=8
x=12
x=16
abs(H_z/H_hor)
φ(H_z/H_hor) (degrees)
zx 3D Model A
zy 3D Model A
zx 2D TM Model
zx 2D TE Model
(d)
T (s)

Fig. 5.

Over the center of the structure, for periods greater than 10 s, ρ_{xy} is almost an order of magnitude lower than ρ_{yx}. Going towards the border of the conductor, ρ_{xy} increases and ρ_{yx} varies very slowly with x. A similar behavior is observed in the apparent resistivities of a 2D model with the same section $y = 0$ as model A.

Comparing the shape of ρ_{xy} curves of the 3D and 2D structures, a near parallel shift between the curves is basically observed for the larger periods, however, the ρ_{yx} curves have different slopes at these periods.

In Figure 4a, the two equivalent 2D models obtained adjusting either ρ_{xy} and ϕ_{xy} (TM model) or ρ_{yx} and ϕ_{yx} (TE model) are shown, together with the corresponding section of model A. The most interesting point to be noted is that these two models are almost coincident (as will be shown later, the same is not valid for model B, which resembles more a 2D structure). In addition, in both models the thickness of the conductive body appears markedly underestimated. This last result can be understood considering that the response of a 3D conductor of finite lateral dimensions is being approximated by the response of a 2D body of infinite length in the y-direction.

Both TM and TE models give similar responses, therefore in Figure 4c, only the fittings obtained from the TM model are shown. Clearly, curves ρ_{xy} and ϕ_{xy} are well fitted for all periods while the ρ_{yx} and ϕ_{yx} fits are acceptable only at periods lower than 10–100 s (this indicates the 3D character of model A). In the table below, the root-mean-square values of the percentual errors (RMSPE) of the apparent resistivities and the root-mean-square values of the errors (RMSE) of the phases, obtained for the TM and TE models, are listed.

	RMSPE (ρ_{xy})	RMSE (ϕ_{xy})	RMSPE (ρ_{yx})	RMSE (ϕ_{yx})
TM model	0.34%	0.93°	51%	28°
TE model	1.0%	3.9°	49%	26°

Forward calculations of the modulus and phase of T_x for the two equivalent 2D models are presented in Figure 4d. These results are surprisingly good, since the vertical field is not used for the fittings. The matches are better for the TE results, because, for a 2D structure, T_x is the element of the tipper associated with the TE mode. As mentioned previously, T_y is always equal to 0 for 2D structures; in addition, due to the existing symmetries, it is also 0 for model A, along the $y = 0$ profile.

Profile $y = 4$ km—The apparent resistivities and phases of model A at $y = 4$ km, and of a 2D structure with the same x-z cross section, are shown in Figure 5b. The behavior of these curves when x is varied, is similar to the one described for the profile $y = 0$. In this case, the curves ρ_{xy} and ϕ_{xy} of the 2D structure draw nearer to the corresponding 3D curves, however, the slopes, the curves ρ_{yx} of the 3D and 2D models are still different for the larger periods.

The thickness of the conductor is fairly well estimated by the 2D modelings. The best result corresponds to the TM model (Fig. 5c). The errors are:

	RMSPE (ρ_{xy})	RMSE (ϕ_{xy})	RMSPE (ρ_{yx})	RMSE (ϕ_{yx})
TM model	0.034%	0.083°	15%	18°
TE model	1.5%	1.6°	22%	11°

The elements of the tippers T_x and T_y are shown in Figure 5d. For this profile, T_y is different from 0 for model A, and its dependence on the period is intimately related to the characteristics of this model. T_y is small at the shorter periods because only the shallow 2D structure is detected and it is also small at the longer periods where the 1D behavior is recovered; for intermediate periods, the value of T_y is comparable to that of T_x, this being a clear indicator of the presence of the 3D body. Once again, the best match between the 3D and 2D T_x values is obtained from the TE model.

Model B

Because the strike direction of the upper 2D structure coincides in this case with the direction of maximum elongation of the deeper 3D conductor, lower 3D effects are expected.

The two profiles considered for this model are profile $y = 0$ (Fig. 6a) and profile $y = 8$ km (Fig. 7a).

Profile $y = 0$—The response of model B at $y = 0$, together with the response of a 2D structure with the same x-z cross section, is plotted in Figure 6b. The differences between the two responses are less than the ones observed for model A. In particular, for the longest periods, the curves ρ_{xy}, ϕ_{xy} and ϕ_{yx} of model B present only a parallel shift with respect to the curves of the 2D structure, and the differences between the slopes of the curves ρ_{yx} are not so great.

Contrary to what is obtained for model A, the equivalent 2D models are not coincident in this case (see Fig. 6a). This difference arises because structure B has more 2D characteristics. Consequently, since the TM mode is more sensitive to lateral variations of the conductivity distribution than the TE mode, the TM model obtained fitting the xy components gives a better estimation of the maximum conductor thickness. Nevertheless, an underestimation of this thickness still occurs.

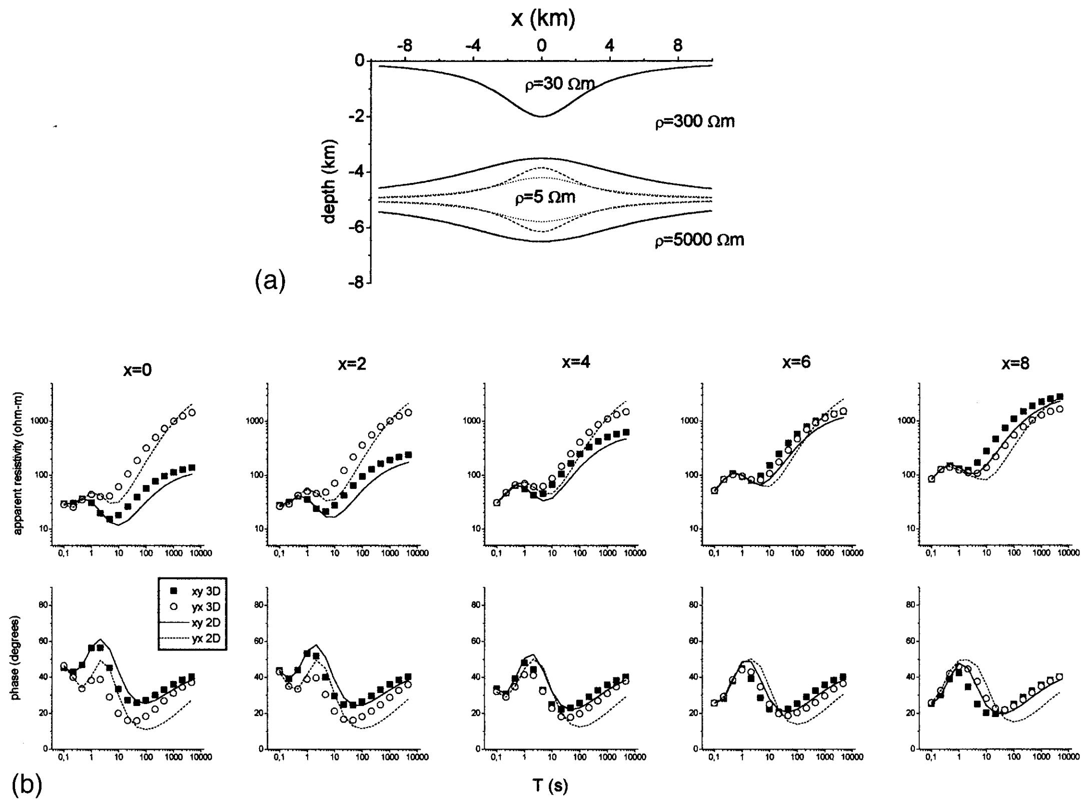

Figure 6

(a) Cross section of Model B at $y = 0$, together with the equivalent 2D models (dashed contours—2D TM model obtained adjusting the 3D xy-component responses; dotted contours—2D TE model obtained adjusting the 3D yx-component responses). (b) 3D apparent resistivity (ρ_{xy} and ρ_{yx}) and phase (ϕ_{xy} and ϕ_{yx}) curves from the corresponding impedance tensor components, at $y = 0$, for different values of x. The responses of a 2D model with the same cross section are also shown. (c) 2D TM model fits of the 3D xy components. Results for the 2D TE model are similar. (d) Comparison of 3D modulus and phase of T_x, with 2D TE forward responses of the TM and TE models.

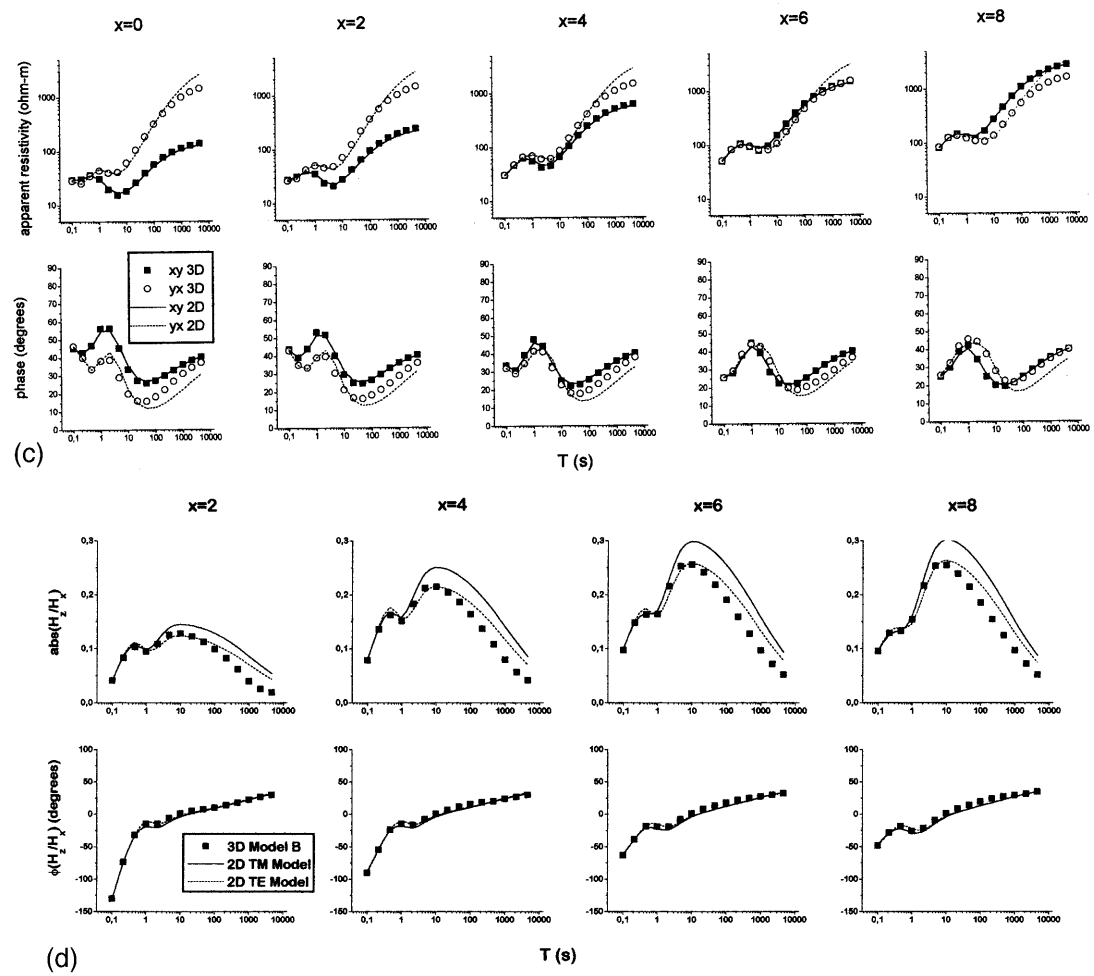

x=0
x=2
x=4
x=6
x=8
apparent resistivity (ohm-m)
phase (degrees)
xy 3D
yx 3D
xy 2D
yx 2D
(c)
T (s)
x=2
x=4
x=6
x=8
abs(H_z/H_x)
φ(H_z/H_x) (degrees)
3D Model B
2D TM Model
2D TE Model
(d)
T (s)

Fig. 6.

The fittings obtained for ρ_{xy} and ϕ_{xy} from the two equivalent 2D models are as good as the ones obtained in the case of the profile $y = 0$ of model A, while the fits of ρ_{yx} and ϕ_{yx} are better in this case, especially at the greater periods. Once more, only the fits obtained from the TM model are plotted (Fig. 6c), because the results for the TE model are similar. Now, the errors are:

	RMSPE (ρ_{xy})	RMSE (ϕ_{xy})	RMSPE (ρ_{yx})	RMSE (ϕ_{yx})
TM model	0.23%	0.92°	16%	16°
TE model	1.0%	3.5°	17%	13°

The best fitting of T_x (Fig. 6d) results from the TE model, for the same reasons as in the former case (Fig. 4d).

According to the results published by WANNAMAKER *et al.* (1984), the xy components of the 3D response of geometrically regular, elongate prismatic conductors, along centrally located transverse profiles, are essentially the same as the TM components of the response of 2D bodies with identical cross sections. Therefore, an accurate modeling of such profiles can be made using 2D, TM algorithms. For the model considered here, the 3D and 2D xy components are not coincident, especially over the body; thereafter, the TM model obtained differs from the actual cross section. This result is partly a consequence of the smooth geometry, since the galvanic effects produced by boundary charges are considerably stronger near the lateral, vertical sides of a prism, than on the sides of the smooth conductor in model B. The differences are also due to a less effective strike length in this model. In addition, this body is buried more than the old plate model, which continues the response upward somewhat. Response decay from 3D upward continuation is faster than 2D decay.

Profile $y = 8$ *km*—For this model, over the border of the conductor, the response is almost coincident with that of a 2D structure with the same x-z cross section (Fig. 7b). The exception is the component of the tipper T_y, which would be equal to 0 in a strictly 2D case (Fig. 7c).

Model C

The types of structures which include a superficial 3D conductive body embedded in a 2D medium have been widely studied and there are several methods which allow consideration of the distortions introduced in the response curves. Generally, the main objective of these methods is not the description of the

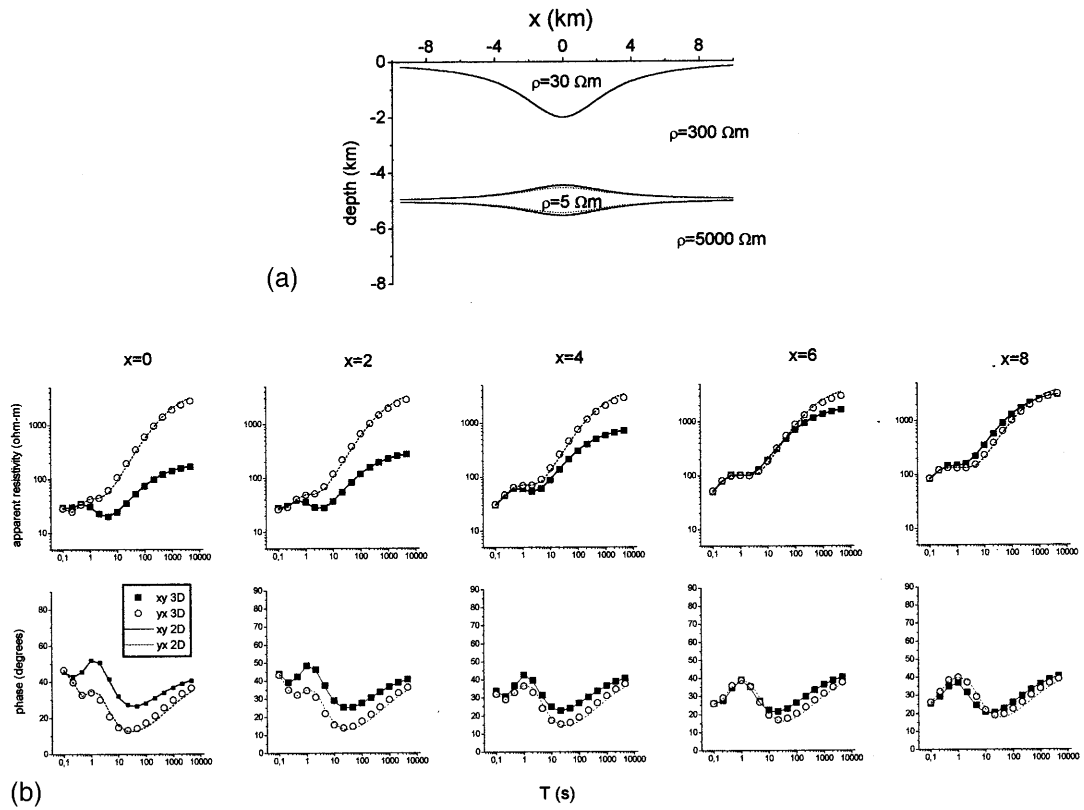

x (km)
depth (km)
ρ=30 Ωm
ρ=300 Ωm
ρ=5 Ωm
ρ=5000 Ωm
(a)
x=0
x=2
x=4
x=6
x=8
apparent resistivity (ohm-m)
phase (degrees)
xy 3D
yx 3D
xy 2D
yx 2D
(b)
T (s)

Fig. 7.

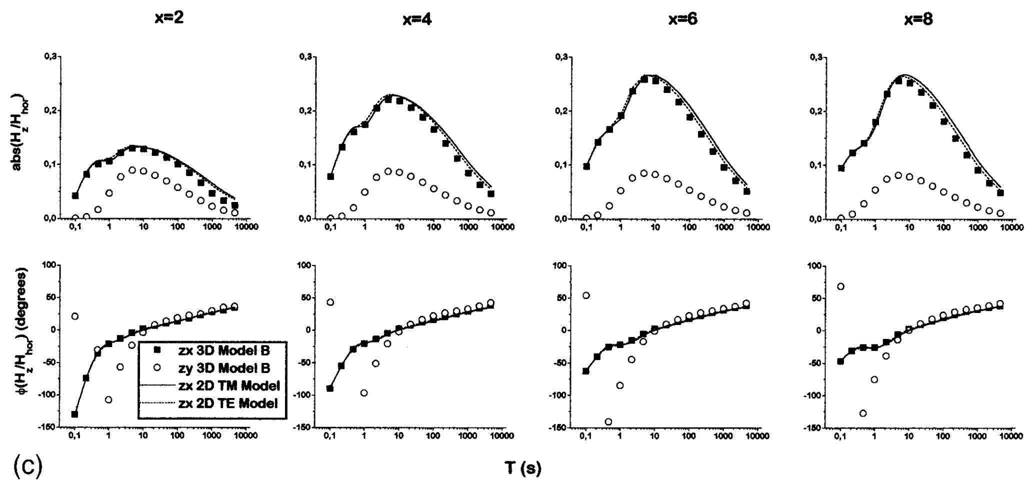

Figure 7

(a) Cross section of Model B at $y = 8$ km, together with the equivalent 2D models (dashed contours—2D TM model obtained adjusting the 3D xy-component responses; dotted contours—2D TE model obtained adjusting the 3D yx-component responses). (b) 3D apparent resistivity (ρ_{xy} and ρ_{yx}) and phase (ϕ_{xy} and ϕ_{yx}) curves from the corresponding impedance tensor components, at $y = 8$ km, for different values of x. The responses of a 2D model with the same cross section are also shown. (c) Comparison of 3D modulus and phase of T_x, with 2D TE forward responses of the TM and TE models.

shallow body but a better knowledge of the underlying 2D structure (e.g., GROOM and BAILEY, 1989).

The RF-3D code is applied here to model the response of a shallow conductive body with smooth contours and the results are again compared with the response of a 2D model with the same cross section (Figs. 8a and b).

From Figure 8b, it is seen that the distortion introduced by the shallow 3D conductor is maximum over the center of the structure. In addition, this distortion is smaller than that obtained for the 2D shallow conductor with the same cross section. It is important to point out that the phases tend to the values corresponding to the TM mode of the 2D model, for periods exceeding approximately 30 s.

A resistive body was also tested, but for this geometry it had a very small response.

In a previous paper, the effects produced by the presence of a vertically anisotropic layer on different 2D configurations were analyzed (OSELLA and MARTINELLI, 1993). The studies indicated that in the case of structures with alternating conductive and resistive layers, these effects decrease strongly as the depth of the anisotropic layer increases. A similar behavior was observed after analyzing different 3D configurations. In particular, for model C and also for a 2D model of the same cross section, only the vertical anisotropy of the first layer can be detected. The magnitude of the observed effect is maximum at $x = 0$ (Fig. 8c) and quickly decreases as x increases.

In 2D cases, vertical anisotropy only distorts the TM response because the vertical electric field is zero in the TE mode. For 3D structures, both the xy and yx components of the response are affected, because the vertical electric field is always non-zero.

At the greater frequencies, since the electric field is nearly horizontal, no effect is observed. Anisotropy becomes important when frequencies are low enough such that skin depth reaches the depth of the buried body. Thereafter, current can actually flow down the anisotropy and connect to the deeper structure before it is dissipated.

Conclusions

The electromagnetic responses due to smooth, elongated conductive bodies underlying a 2D structure are analyzed using the RF-3D code. Two models considered are Model A, with the direction of maximum elongation perpendicular to the strike direction of the 2D structure, and Model B, with the body aligned with the shallow structure. The main results can be summarized as follows.

For both models (A and B), when equivalent 2D, TM and TE models are obtained adjusting, respectively, the xy or the yx-components of the 3D response,

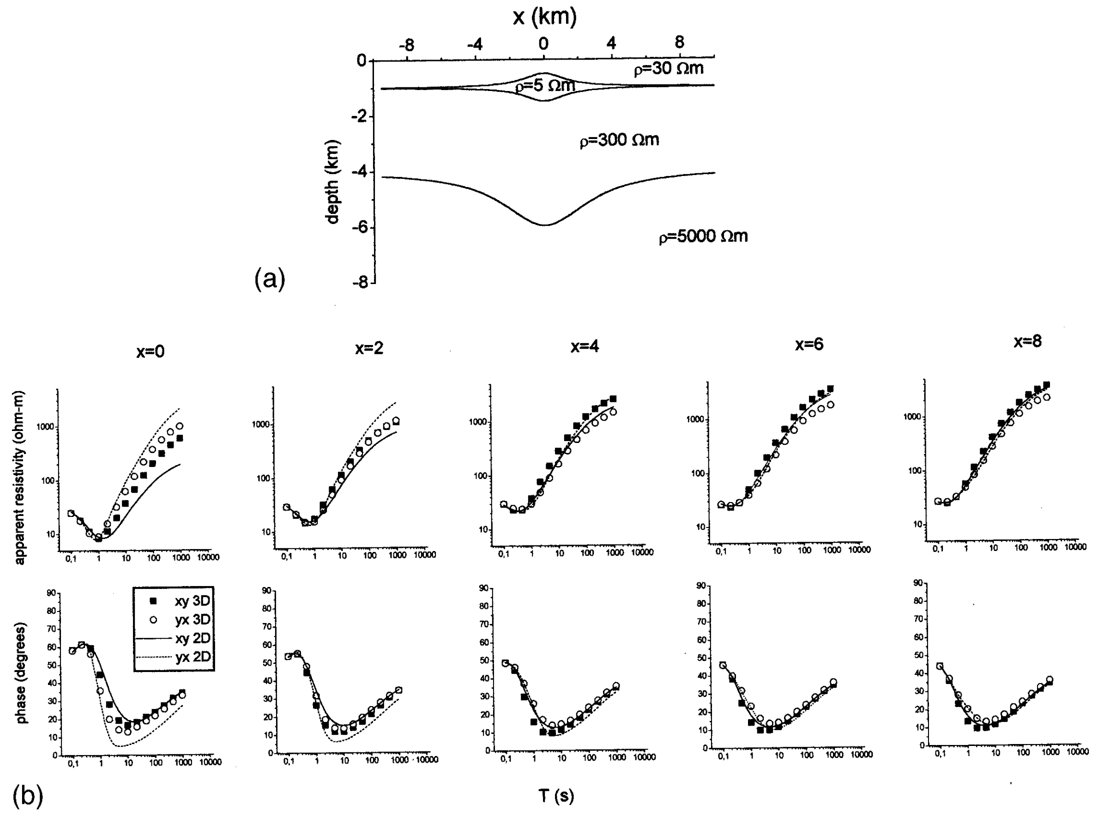
x (km)
-8
-4
0
4
8
0
-2
-4
-6
-8
depth (km)
ρ=30 Ωm
ρ=5 Ωm
ρ=300 Ωm
ρ=5000 Ωm
(a)
x=0
x=2
x=4
x=6
x=8
apparent resistivity (ohm-m)
phase (degrees)
xy 3D
yx 3D
xy 2D
yx 2D
(b)
T (s)

Fig. 8.

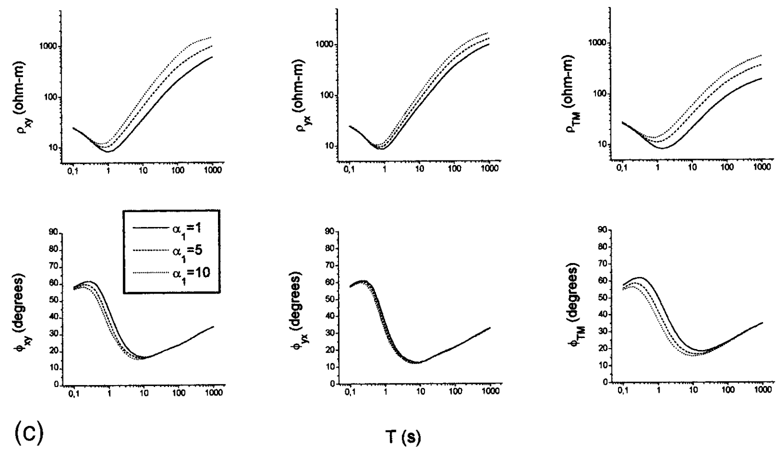

Figure 8

(a) Cross section of Model C at $y = 0$. (b) 3D apparent resistivity (ρ_{xy} and ρ_{yx}) phase (ϕ_{xy} and ϕ_{yx}) curves from the corresponding components of the impedance tensor, at $y = 0$, for different values of x. The responses of a 2D model with the same cross section are also shown. (c) Effect of vertical anisotropy in the first layer, at $x = 0$. $\alpha = \sigma_h/\sigma_v$ is the measure of anisotropy inside layer 1.

a good fit is always obtained for the *xy* component. The fitting of the *yx* component is poor, especially at the larger periods; the worst results correspond to the case of model A.

For model A, the TM and TE model responses are similar, and they both underestimate the thickness of the conductor by about 30%. For model B, which is more 2D-like, the TM model gives the best approximation to the actual structure. Nevertheless, in this model, conductor thickness also appears undervalued by 24%.

For geometrically regular, elongate, prismatic conductors, accurate cross sections can be inferred from 2D, TM modeling of the *xy* components of the 3D response, along centrally located, transverse profiles. Subsequently, the major differences obtained in this study between the resulting TM models and the actual cross sections, particularly in the case of model B, are partly a consequence of the smooth geometry. This is because the galvanic effects produced by boundary charges are substantially stronger near the vertical sides of a prism than on the smooth, tapered sides of the conductors considered here. The differences are also due to a less effective strike length in the models. In addition, these bodies are buried more than the old plate model, which continues the responses upward somewhat. Response decay from 3D upward continuations is faster than 2D decay.

It can be added that different tests have been performed assuming resistive bodies, however they produced very small responses. Vertical anisotropy of the bodies, either those resistive or conductive, also had no effect on the response.

For a smooth superficial body over a 2D regional structure (Model C), only the vertical anisotropy of the first layer can be detected, as a shift (properly an overestimation) of the apparent resistivity curves at the longer periods.

Acknowledgements

This work was supported by Conicet and the University of Buenos Aires.

References

BAHR, K. (1988), *Interpretation of the Magnetotelluric Impedance Tensor: Regional Induction and Local Telluric Distortion*, J. Geophys. Res. *62*, 119–127.

BOERSMA, J. R., and JIRACEK, G. R. (1987), *Three-dimensional Magnetotelluric Modeling with the Rayleigh-FFT Method*, Internat. Union of Geodesy and Geophysics General Assembly, Vancouver, Canada, Abs. 1452.

CAGNIARD, L. (1953), *Basic Theory of the Magnetotelluric Method of Geophysical Prospecting*, Geophysics *18*, 605–635.

DANIYAN, M. A., and PEEPLES, W. J. (1986), *Application of Rayleigh-FFT Technique to Three-dimensional Magnetotelluric Interpretation*, Annales Geophysicae *4B*, 441–456.

GROOM, R., and BAILEY, R. (1989), *Decomposition of Magnetotelluric Impedance Tensors in the Presence of Local Three-dimensional Galvanic Distortion*, J. Geophys. Res. *94*, 1913–1925.

HOHMANN, G. W. (1975), *Three-dimensional Induced Polarization and Electromagnetic Modeling*, Geophys. *40*, 309–324.

JIRACEK, G. R., REDDIG, R. P., and KOJINA, R. K. (1989), *Application of the Rayleigh-FFT Technique to Magnetotelluric Modeling and Correction*, Phys. Earth Planet. Int. *53*, 365–375.

LIPPMANN, B. A. (1953), *Note on the Theory of Gratings*, J. Opt. Soc. Am. *43*, 408–414.

MACKIE, R., MADDEN, T., and WANNAMAKER, P. (1993), *Three-dimensional Magnetotelluric Modeling Using Difference Equations. Theory and Comparisons to Integral Equation Solutions*, Geophys. *58*, 215–226.

MARTINELLI, P., and OSELLA, A. (1997), *MT Forward Modeling of 3D Anisotropic Electrical Conductivity Structures Using the Rayleigh-Fourier Method*, J. Geomag. Geoelectr. *49* (11), 1499–1518.

MILLER, R. F. (1971), *On the Rayleigh Assumption in Scattering by a Periodic Surface*, Proc. Cambridge Phyl. Soc. *69*, 217–225.

MOGI, T. (1996), *Three-dimensional Modeling of Magnetotelluric Data Using Finite Element Method*, J. Appl. Geophys. *35*, 185–189.

OSELLA, A., and MARTINELLI, P. (1993), *Magnetotelluric Response of Anisotropic 2-D Structures*, Geophys. J. Inter. *115*, 819–828.

SMITH, J. T. (1996), *Conservative Modeling of 3-D Electromagnetic Fields. Paper I: Properties and Error Analysis*, Geophysics *61*(5), 1308–1318. *Paper II: Biconjugate Gradient Solution and an Accelerator*, Geophysics *61*(*5*), 1319–1324.

SMITH, J. T., and BOOKER, J. (1991), *Rapid Inversion of Two and Three-dimensional Magnetotelluric Data*, J. Geophys. Res. *96*, 3905–3922.

WANNAMAKER, P. E., HOHMANN, G. W., and WARD, S. H. (1984), *Magnetotelluric Responses of Three-dimensional Bodies in Layered Earths*, Geophysics *49*, 1517–1533.

WANNAMAKER, P., STODT, J., and RIJO, L. (1987), *A Stable Finite Element Solution for Two-dimensional Magnetotelluric Modeling*, Geophys. J. R. Astr. Soc. *88*, 277–296.

WANNAMAKER, P. (1991), *Advances in Three-dimensional Magnetotelluric Modeling Using Integral Equations*, Geophys. *11*, 1716–1728.

(Received July 15, 1998, accepted June 7, 1999)

.